University of Massachusetts Boston

ScholarWorks at UMass Boston

Physics Faculty Publications

Physics

12-13-2004

Medical image processing using transient Fourier holography in bacteriorhodopsin films

Sri-Rajasekhar Kothapalli
University of Massachusetts Boston

Pengfei Wu
University of Massachusetts Boston

Chandra S. Yelleswarapu
University of Massachusetts Boston, chandra.yelleswarapu@umb.edu

D.V.G.L.N. Rao
University of Massachusetts Boston, raod@umb.edu

Follow this and additional works at: http://scholarworks.umb.edu/physics_faculty_pubs

Part of the Optics Commons

Recommended Citation

Kothapalli, Sri-Rajasekhar; Wu, Pengfei; Yelleswarapu, Chandra S.; and Rao, D.V.G.L.N., "Medical image processing using transient Fourier holography in bacteriorhodopsin films" (2004). *Physics Faculty Publications.* Paper 3.
http://scholarworks.umb.edu/physics_faculty_pubs/3

Medical image processing using transient Fourier holography in bacteriorhodopsin films

Sri-Rajasekhar Kothapalli, Pengfei Wu, Chandra S. Yelleswarapu, and D. V. G. L. N. Rao

Related Articles

An excitation wavelength–scanning spectral imaging system for preclinical imaging
Rev. Sci. Instrum. 79, 023707 (2008)

Terahertz imaging diagnostics of cancer tissues with a chemometrics technique
Appl. Phys. Lett. 90, 041102 (2007)

Small angle scattering signals for (neutron) computerized tomography
Appl. Phys. Lett. 85, 488 (2004)

Wide-field, real-time depth-resolved imaging using structured illumination with photorefractive holography
Appl. Phys. Lett. 81, 2148 (2002)

Imaging ferromagnetic tracers with an ac biosusceptometer
Rev. Sci. Instrum. 71, 2532 (2000)

Additional information on Appl. Phys. Lett.

Medical image processing using transient Fourier holography in bacteriorhodopsin films

Sri-Rajasekhar Kothapalli, Pengfei Wu, Chandra S. Yelleswarapu, and D. V. G. L. N. Rao[a]
Department of Physics, University of Massachusetts, Boston, Massachusetts, 02125

Real time image processing is demonstrated by recording and reconstructing the transient photoisomerizative grating formed in the bR film using Fourier holography. Desired spatial frequencies including both high and low band in the object beam are reconstructed by controlling the reference beam intensity. The results are in agreement with a theoretical model based on photoisomerization grating. We exploit this technique to process mammograms in real-time for identification of microcalcifications buried in the soft tissue for early detection of breast cancer. A feature of the technique is the ability to transient display of selected spatial frequencies in the reconstructing process which enables the radiologists to study the features of interest. © *2004 American Institute of Physics.* [DOI: 10.1063/1.1833567]

Real-time optical information processing using nonlinear optical materials has received considerable attention recently due to ever increasing demand for processing a huge amount of data.[1–3] Photorefractive materials are widely used for implementation of optical Fourier transform operations such as edge enhancement, band pass filtering, noise removal, and pattern recognition.[4,5] There is much scientific interest in photoisomerizative biological and organic molecules for studies on optical nonlinearity[6] and applications in photonics such as optical storage,[1] switching,[7] and information processing.[8] Small molecular size with resulting high resolution and low driving energy make them an ideal choice for applications in optical image processing as compared to the inorganic photorefractive materials. The biological photochrome bacteriorhodopsin shows many intrinsic optical and physical properties[9] and is receiving much attention as an alternative to conventional photorefractive materials for applications in optical recording and image processing. The spatial filtering in bR was performed using a control beam that precisely manipulates spatial frequencies exploiting saturable absorption[10] and photoinduced aniosotropy.[8] As compared to other materials like photorefractive crystals, the bR films have many advantages such as high spatial resolution of over 6000 lines/mm,[11] high photoisomerization efficiency, ease of preparation of thin films of large area, and reversibility of use.

In this letter, we study transient Fourier holographic gratings based on photoinduced isomerization properties of bR films. The desired spatial frequency components in the Fourier transformation of the object can be selected by matching their intensity to that of the reference beam. We used this technique to process mammograms in real-time for identification of microcalcifications buried in the soft tissue. The results offer useful information to radiologists for early detection of breast cancer. An added advantage is that the radiologist can compare the processed image and original image in real-time by blocking and unblocking the object beam.

Figure 1 shows the experimental arrangement of Fourier holography for study of transient nonlinear spatial filtering and applications of image processing. The 568 nm output

from an Ar–Kr ion laser is expanded by a beam expander (BE), and then split into two beams by a 50–50 beam splitter BS_1. The object beam passing through an object (mammogram or binary object E), is transformed to Fourier plane by a lens L_1 with focal length of 20 cm. At the Fourier plane the bR film is placed for real-time processing of spatial frequency information contained in the object. The Fourier spectrum of the object contains low spatial frequencies at the center with high intensity and high spatial frequencies at the edge with low intensities. The bR film, wild-type purchased from Munich Innovative Biomaterials GmbH, has optical density of about 5 at 570 nm with a thickness of about 100 μm. The reference beam overlaps the Fourier transform of the object beam on the bR film using beam splitter BS_2 thereby recording a Fourier hologram. A small angle of about 5° between reference and object beams is set to give maximum diffraction efficiency. A variable attenuator (VA) is placed in the reference path to match its intensity to that of the desired spatial frequency band in Fourier spectrum of the object beam. It takes about 5 s to saturate the grating with optimum modulation and the hologram is completely recorded. When the object beam is blocked, for the readout process, the reference beam performs the reconstruction of the recorded Fourier hologram. During the readout process the reference beam erases (in about 10 s) the contrast in the population grating and thus bR film is brought back to its original state with no history of object information and is ready for the next cycle. The desired frequency band of the object wave reconstructed from the hologram passes through the lens L_2 with an inverse Fourier transform configuration and is imaged on to the CCD camera.

Initially we investigated temporal and intensity-dependent properties of holographic grating recorded by us-
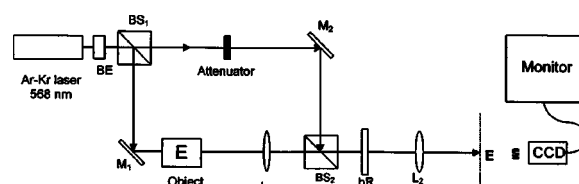

FIG. 1. Experimental arrangement for study of edge enhancement using transient Fourier hologram recorded in bR film. M: mirrors; BS: beam splitters; and L: lenses.
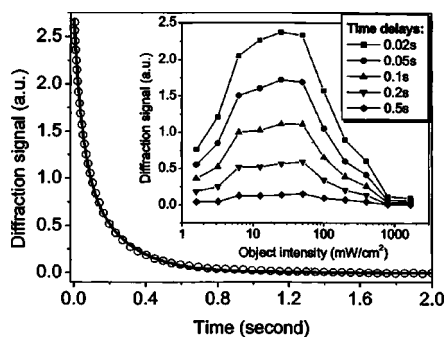
[a]Electronic mail: raod@umb.edu

FIG. 2. Experimental results of temporal decay of diffraction signal at matched object and reference beam intensity of 26 mW/cm^2. The solid line is the theoretical fit. Inlet: diffraction signal as a function of object beam intensity for various time delays with fixed reference beam intensity of 26 mW/cm^2.

ing bR films. For this study we slightly modified the experimental setup shown in Fig. 1. The object and Fourier transform lenses are removed from the object path and the CCD camera is replaced by a photodetector. The intensity in the reference beam is fixed at 26 mW/cm^2 while intensity in the object beam is varied from 1.6 mW/cm^2 to 1.6 W/cm^2, to stimulate the range of intensities of spatial frequencies in the Fourier spectrum of the object. The holographic grating formed due to the interference between the two beams is recorded in bR film for about 5 s to reach its saturation. The optimum of diffraction efficiency occurs when object beam intensity is matched to the reference beam intensity. When the object beam is blocked, the reference beam decreases the grating contrast decreases due to isomerization process from M to B resulting in decay of the diffracted signal. Figure 2 shows the decay of diffraction signal with time for an object beam intensity of 26 mW/cm^2 and matched reference beam intensity of same value. We observed decay of the diffraction signal for a series of object beam intensities. The values of diffraction signals obtained from this data are plotted as a function of object beam intensities for various time delays shown in Fig. 2 inlet. It is clear that the diffraction efficiencies show optimum values when the object beam intensity matches the reference beam. At either low or high intensity region of the object beam, the diffraction efficiency decreases.

The experimental results can be understood using the mechanism of photoinduced isomerization grating formed in bR film. Upon excitation of the initial B state (all trans), the bR molecule goes through several intermediate states with short lifetimes to the relatively long-lived M state (*cis*) and relaxes back to the initial state spontaneously.[12] We may consider only the B and M states as the other intermediate states in the photocycle are short lived. The initial B state has an absorption peak at 570 nm while the long-lived M state has an absorption peak at 412 nm.

Monochromatic plane waves are used to form holographic grating in bR film. Thus, the bR molecules simply undergo photoisomerization process as follows:

$$\text{B} \underset{R_2, R_T}{\overset{R_1}{\rightleftarrows}} \text{M},$$
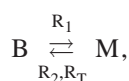
where R_i is the rate of the photoisomerization, $i=1$ and 2 corresponding to the photoisomerizations from B→M (trans to cis) and M→B (cis to trans) respectively while R_T is the rate of the thermal isomerization from M→B. Due to the

spatial intensity modulation induced by the interference of the two recording beams in the sample, the photoisomerization from B→M is spatially modulated leading to a M state population grating. The diffraction efficiency of this grating is proportional to the square of modulated contrast of the M state population grating. Following the theoretical model for biphoton grating in azo materials,[13] we express the temporal behavior of the modulated contrast in the reading process as

$$\Delta N_2(t) = \frac{(A_1 A_2)IN_0}{\left[1+(A_1+A_2)I\right]^2} e^{-(1+A_2I)R_T t}, \tag{1}$$

where N_0 is the total number of bR molecules given by $N_0 = N_1(t) + N_2(t)$, $N_1(t)$ and $N_2(t)$ being the temporal populations of the M and B, respectively. $R_i/R_T = A_i I$, where $A_i = \sigma_i \phi_i / \hbar \omega R_T$, σ_i is the absorption cross section of the B state (i=1) or M-state (i=2), ϕ_i is the quantum yield of photoisomerization from B→M state (i=1) and M→B (i=2) and ω is the angular frequency of the light. From the Eq. (1) it follows that the dependence of both the grating contrast and decay time of diffraction signal on reference beam intensity I is in agreement with our experimental observation. In addition, our experimental results of the diffraction decay can be explained in terms of two lifetimes. For example, theoretical plot (solid line) in Fig. 2 is obtained using two lifetimes, 62 and 240 ms. We believe the short one originates from the isomerization rate from M→B, and the long one is due to the mechanism of bR molecular reorientation. We modified Eq. (1) with two exponential decays corresponding to these two lifetimes to fit the experimental data in Fig. 2. Diffraction decay data for other object intensities can also be explained similarly.

The intensity in Fourier spectrum of any object is spatially distributed—low frequencies are at high intensity and high frequencies are at low intensity. We exploit the temporal and intensity dependent features of diffraction efficiency of bR sample for selective recording of spatial frequencies for applications in image processing. To illustrate the feasibility of the technique we first recorded high spatial frequency components of a binary object E, by matching the corresponding intensity to the intensity of the reference beam. The recording process takes about 5 s so that the contrast of Fourier hologram reaches its maximum in the bR film. When the object beam is blocked, the reconstructed wave by the reference beam shows an edge enhancement effect. The experimental results are shown in Fig. 3(b). In addition, the bR material also has saturable absorption feature which enables it to directly pass low-frequency components of the image and block high-frequency components. In the absence of reference beam, an image with soft edge of object E as shown in Fig. 3(c) is obtained. Thus this scheme is able to give the processed results of both low-frequency and high-frequency components in real time and can be adopted for other frequency bands as well.

We now exploit this scheme for processing mammograms for detection of microcalcifications. The microcalcifications (tiny calcium deposits in human breast) correspond to high spatial frequencies in the Fourier spectrum because of their small size ($\sim 10~\mu$m) and diffuse nature. The object E in the above experiment is replaced with region of interest (ROI marked by the radiologist) of the mammogram as depicted in Fig. 3(d). By controlling the reference intensity, edge enhancement of mammograms is achieved leading to

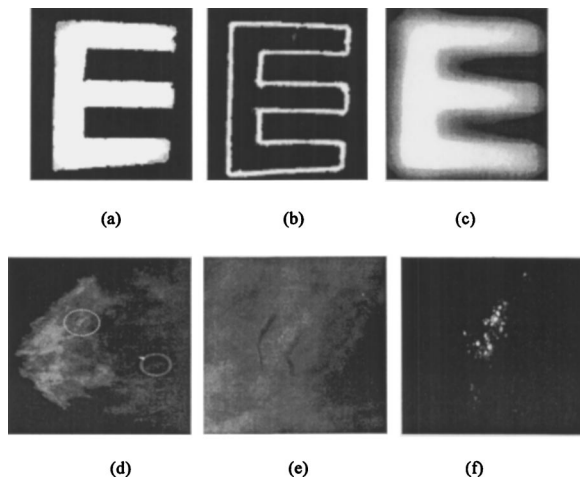(a)   (b)   (c)

(d)   (e)   (f)

FIG. 3. Experimental results of image processing using Fourier holography. For the binary image "E": (a) original, (b) edge-enhanced, and (c) edge-softened. For the mammograms: (d) original image with of region of interest (ROI) circled by radiologists, (e) blowup of the ROI; (f) processed image showing calcifications.

(a)   (b)

FIG. 4. Transient display of spatial frequency information of grating resolution chart captured at times (a) t=0 and (b) t=5 s.

clear display of microcalcifications (not visible to the naked eye of the radiologist) on the monitor as shown in Fig. 3(f). Irrespective of different size of regions of interest and density of soft tissue present in mammograms, the radiologist can easily scan for desired microcalcification clusters by rotating the variable attenuator placed in the path of the reference beam. With the spatial resolution of bR film ($\sim$ 6000 lp/mm)[11] and CCD camera resolution ($\sim$67 lp/mm) we could easily detect microcalcifications of $\sim$10 μm in size (10–12 lp/mm).

An additional attractive feature of this technique is the transient nature in display of different spatial frequencies in the Fourier spectrum of an object. Abnormalities detected in mammography are classified as spiculated masses, stellate lesions, circumscribed masses, and microcalcifications. As these abnormalities vary in size and intensity they correspond to different spatial frequency bands in the Fourier spectrum of the mammogram. From the inlet in Fig. 2 we can infer that at a given time, all the spatial frequencies exist with different diffraction efficiencies. The maximum efficiency occurs for a selected band of frequencies that are optimized by matching the intensities of the object and reference beams. Other spatial frequencies also appear but are lower intensity. The dominant frequency band persists for a relatively longer time whereas the other frequencies decay fast. Thus we can distinguish between different spatial frequencies as they reveal at different times. We recorded a movie of the whole hologram recording and readout process using a fast CCD so that the readout process can revisit as well as freeze the frames for the radiologist to concentrate on a particular band of frequencies. To demonstrate this concept we used a resolution chart (USAF negative target, Edmund Optics). As shown in Fig. 4(a) at time t=0 we can observe all the frequency groups [(A) low frequency group, (B) middle frequency group, and (C) high frequency group] but at time at t=5 only the frequency group B which matches the reference beam intensity remains clear while other frequency groups vanish. The radiologist also has the choice of selecting the dominant frequency band by varying the reference beam intensity durin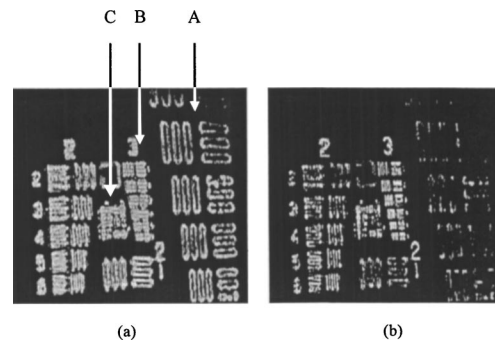g the whole process. This could be a potential advantage to the radiologist in diagnostics of abnormalities in the mammogram that occur at different scales – such as clusters of microcalcifications at small scales, edges of smooth or star-shaped objects in the breast at middle scales and architectural distortions at large scales.[14]

In conclusion, interesting results on temporal and intensity-dependent properties of Fourier holographic gratings using bR films are reported. The analysis using a theoretical model based on photoinduced isomerization agrees with our experimental results. We exploit this technique to process mammograms in real-time for detection of microcalcifications buried in the background of soft tissue. The results are useful to radiologists for early diagnostics of breast cancer. In addition, we found that the information in static processed images can be further separated in time scales. These temporal image features offer useful information to the radiologist about the pathological changes in the image which cannot be obtained from the static processed image. This optical technique can be easily adopted for processing digital mammograms by replacing the object in Fig. 1 with SLM connected to the computer.

[1]J. F. Heanue, M. C. Bashaw, and L. Hesselink, Science **265**, 749 (1994).
[2]J. W. Goodman, Opt. Photonics News **2**, 11 (1991).
[3]R. H. Berg, S. Hvilsted, and P. Ramanujam, Nature (London) **383**, 505 (1996).
[4]J. P. Huignard and J. P. Herriau, Appl. Opt. **17**, 2671 (1978).
[5]T. Y. Chang, J. H. Hong, and P. Yeh, Opt. Lett. **15**, 743 (1990).
[6]D. Dantsker, J. Nonlinear Opt. Phys. Mater. **5**, 775 (1996).
[7]P. Wu, D. V. G. L. N. Rao, B. R. Kimball, M. Nakashima, and B. S. DeCristofano, Appl. Phys. Lett. **81**, 3888 (2002).
[8]J. Joseph, F. J. Arnanda, D. V. G. L. N. Rao, J. A. Akkara, and M. Nakashima, Opt. Lett. **21**, 1499 (1996).
[9]R. R. Birge, Sci. Am. **3**, 90 (1995).
[10]R. Thoma, N. Hampp, C. Brauchle, and D. Oesterhelt, Opt. Lett. **16**, 651 (1991).
[11]Z. Yuan, Y. Bao-Li, W. Ying-Li, M. Neimule, L. Ming, C. Guo-Fu and N. Hampp, Chin. Phys. Lett. **20**, 671 (2003).
[12]A. Lewis, Y. Albeck, Z. Lange, J. Benchowski, and G. Weizman, Science **275**, 1462 (1997).
[13]P. Wu, L. Wang, J. Xu, B. Zou, X. Gong, G. Zhang, G. Tang, and W. Chen, Phys. Rev. B **57**, 3874 (1998).
[14]H. S. Wong, L. Guan, and H. Kong, Proceedings of the 1995 International Conference on Image Processing, ICIP '95, 21.